Acta Cryst. (1971). A27, 134

Convergence of Lattice Sums Encountered in Computing the Scattering of X-rays by Crystal Defects*

BY D. T. KEATING AND A. N. GOLAND

Brookhaven National Laboratory, Upton, New York, 11973, *U.S.A.*

(*Received* 10 *March* 1970)

The diffuse scattering of X-rays from a crystal containing defects involves a sum over all lattice points. This sum suffers from problems in convergence and truncation. These problems are investigated with a computer using the model of a simple cubic lattice containing a body-centered interstitial with a displacement field $\mu = C\mathbf{r}/r^3$. Convergence is discussed in terms of a truncation parameter. Truncating the sum introduces a ripple which is removed when the finite resolution imposed by any measurement is taken into account. Both the truncation parameter and finite resolution determine distances in the lattice. The resolution distance dictates the choice of truncation distance and this is discussed for a Gaussian resolution function. We compare the results of the sum formulation with a commonly used integral approximation. Finally, we find that when the displacements produced by the defect are large the Huang scattering dominates the size-effect scattering and that in this case the diffuse scattering is more intense on the side of a reflection furthest from the origin.

1. Introduction

The diffuse scattering of X-rays from a crystal containing defects involves a sum over all lattice points. The function to be summed is

$$\exp\{i\boldsymbol{\kappa}\cdot\mathbf{r}_n\}(\exp\{i\boldsymbol{\kappa}\cdot\boldsymbol{\mu}_n\}-1),$$

where $\boldsymbol{\kappa}$ is the difference between the incoming and scattered wavevectors, $\mathbf{r}_n$ is the vector to the *nth* lattice point and $\boldsymbol{\mu}_n$ is its vector displacement (Keating, 1968). In practice, evaluation of this sum suffers from convergence and truncation errors. We have investigated these problems with a computer using the model of a simple cubic lattice containing a body-centered interstitial with a displacement field, $\boldsymbol{\mu}_n = C\mathbf{r}_n/r_n^3$, where C is the defect strength (Eshelby, 1954). Our model is that employed by Martin (1960). Results have been obtained in terms of a truncation parameter ε which is the ratio of the magnitude of the smallest displacement retained in the sum to the largest displacement. We have found that the diffuse scattering in those regions of reciprocal space readily accessible to measurement is reasonably stationary, to within $\sim 15\%$, for values of $\varepsilon < 10^{-3}$. For the model this implies summing over 10^5 atoms or more. Although our expression for the diffuse intensity cannot be shown to converge in general, the expression one obtains taking into account finite experimental resolution can be shown to converge. Both the truncation parameter and the instrumental resolution determine distances in the lattice, and the resolution dictates the choice of truncation parameter. We discuss this for a Gaussian resolution function. If $\boldsymbol{\kappa}\cdot\boldsymbol{\mu}_n$ is small then $(\exp\{i\boldsymbol{\kappa}\cdot\boldsymbol{\mu}_n\}-1)$ is often approximated by $i\boldsymbol{\kappa}\cdot\boldsymbol{\mu}_n$ and the sum, being a Fourier transform, is evaluated using Ewald's (1938) integral transformation formula following Ekstein (1949). Using two very different values of the strength we have compared this approximation with the results for the sums. Close to the Bragg reflections the agreement between the two methods is satisfactory for the smaller strength, but is considerably poorer for the larger strength. It is well known that the asymmetry in the diffuse scattering about a Bragg reflection is produced by the so called 'size effect term' (Borie 1957, 1959; Goland & Keating 1968) and depends on the sign of the strength and the Miller indices of the Bragg reflection (Cochran, 1956). However, given a strength of sufficient magnitude, the diffuse scattering is always asymmetric, with the intensity always more intense on the side of the reflection furthest from the origin. For large displacements this is explained by the fact that the Huang scattering (Huang, 1947) which has this symmetry completely dominates the size-effect scattering.

Methods and results

For our model the intensity of the diffuse scattering is given by*

$$I(\kappa) \propto \left|1+\sum_{r\neq 0}^{R(\varepsilon)} \exp\{i\boldsymbol{\kappa}\cdot\mathbf{r}\}(\exp\{iC\boldsymbol{\kappa}\cdot\mathbf{r}/r^3\}-1)\right|^2 . \quad (1)$$

$R(\varepsilon)$ is the truncation distance determined by the truncation parameter ε. Values of $R(\varepsilon)$ for various values of ε considered are listed in Table 1. For our centrosymmetric model we can write

* Work performed under the auspices of the U.S. Atomic Energy Commission.

* See Keating (1968), equation (32). Here $p \ll 1$, and $f_A = f_B$.

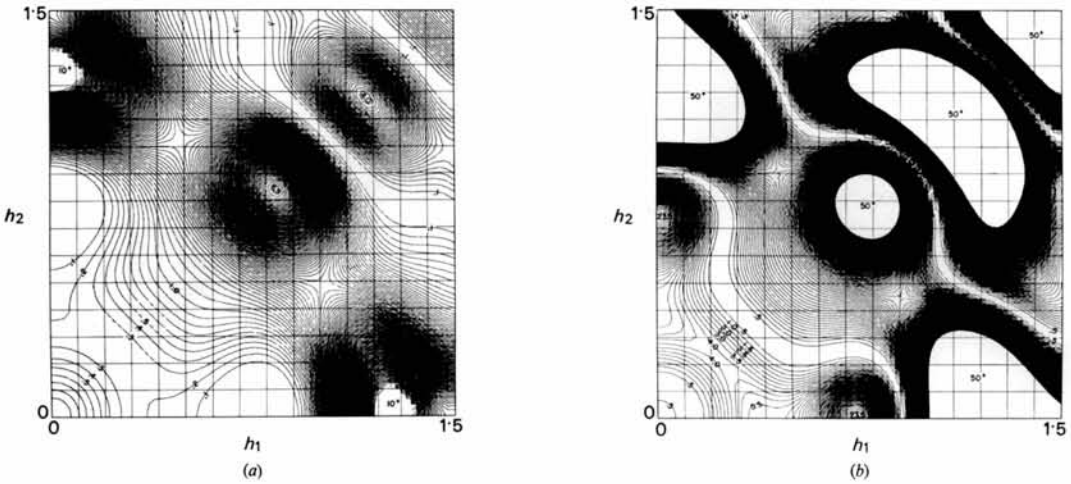

Fig. 1. Contours of diffuse scattering for $R(\varepsilon)=1{\cdot}66a$. (*a*) $4Ca^{-3}=0{\cdot}15$, (*b*) $4Ca^{-3}=0{\cdot}90$.

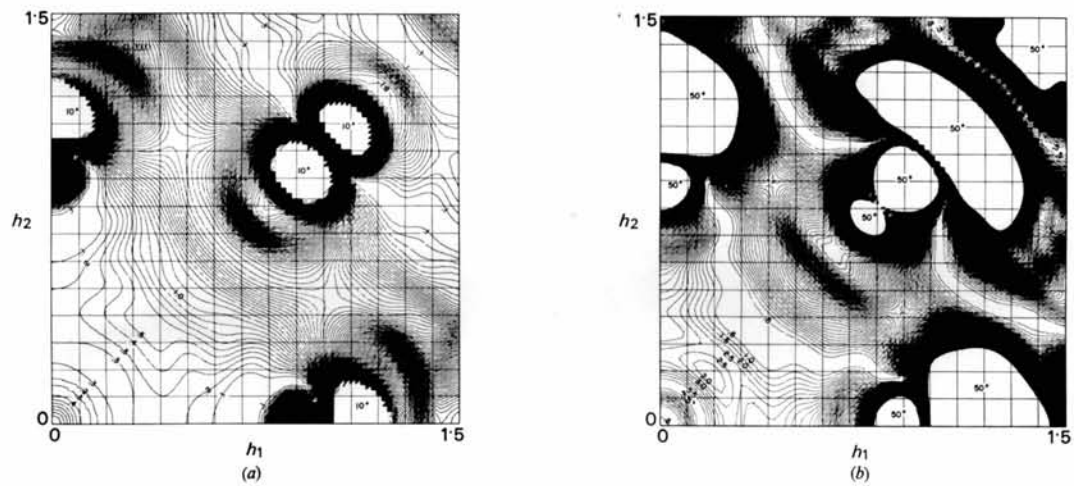

Fig. 2. Contours of diffuse scattering for $R(\varepsilon)=4{\cdot}77a$. (*a*) $4Ca^{-3}=0{\cdot}15$, (*b*) $4Ca^{-3}=0{\cdot}90$.

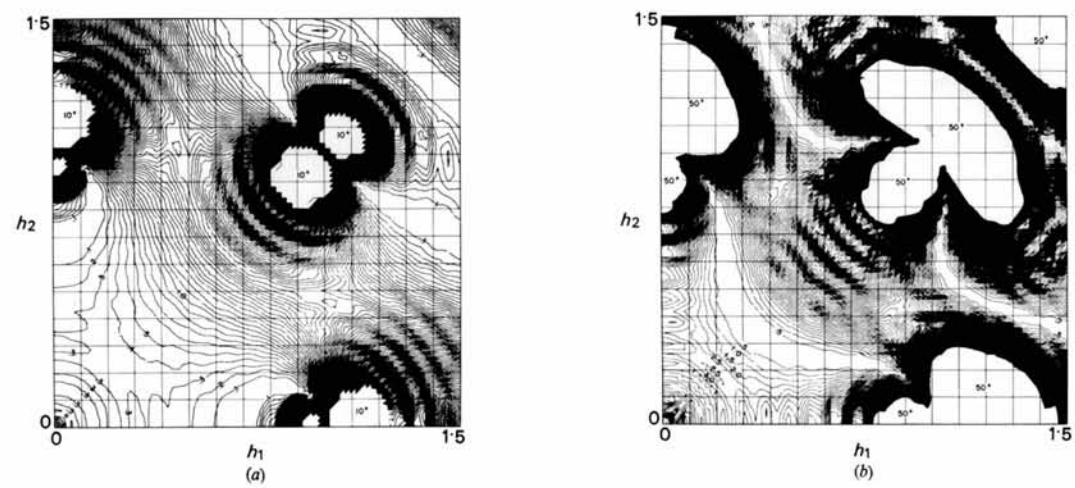

Fig. 3. Contours of diffuse scattering for $R(\varepsilon)=12{\cdot}5a$. (*a*) $4Ca^{-3}=0{\cdot}15$, (*b*) $4Ca^{-3}=0{\cdot}90$.

[*To face p.* 134

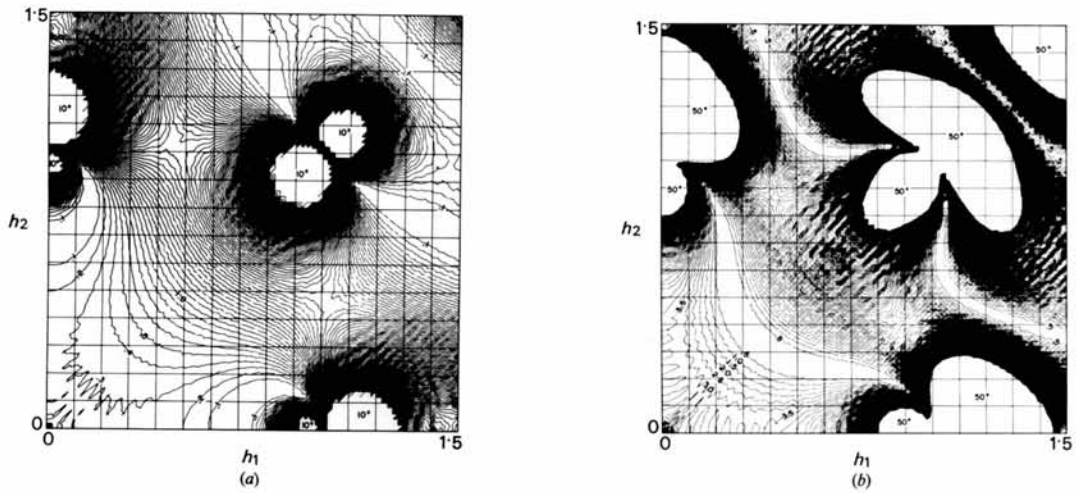

Fig. 4. Contours of diffuse scattering for $R(\varepsilon)=31{\cdot}8a$. (*a*) $4Ca^{-3}=0{\cdot}15$, (*b*) $4Ca^{-3}=0{\cdot}90$.

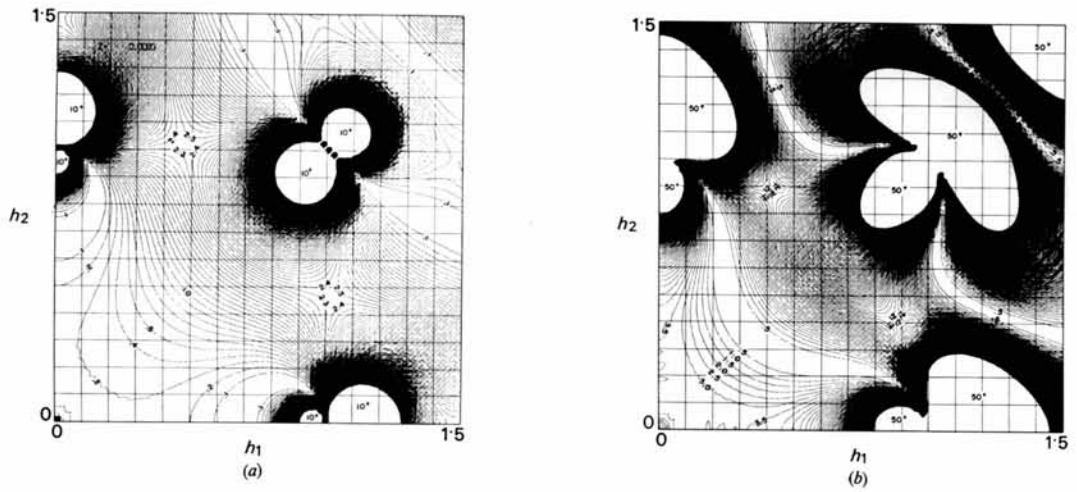

Fig. 5. Contours of diffuse scattering taking into account a finite resolution $R(\sigma)=15{\cdot}9a$, $R(\varepsilon)=31{\cdot}8a$. (*a*) $4Ca^{-3}=0{\cdot}15$, (*b*) $4Ca^{-3}=0{\cdot}90$.

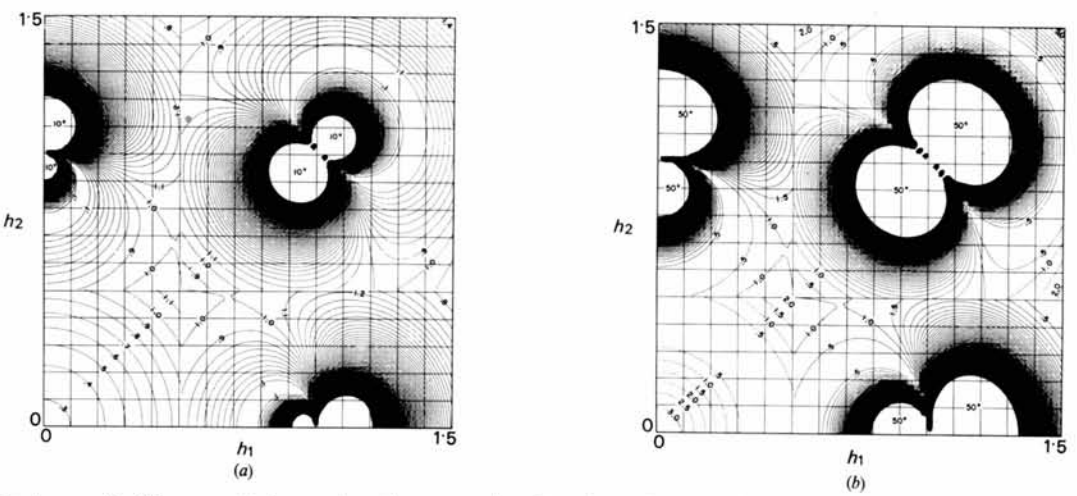

Fig. 6. Contours of diffuse scattering using the approximation formula, equation (10). (*a*) $4Ca^{-3}=0{\cdot}15$, (*b*) $4Ca^{-3}=0{\cdot}90$.

$$I(h_1h_2h_3) \propto \{1-2\sum_{l_1}\sum_{l_2}\sum_{l_3}\sin[4\pi C(La)^{-3}(l_1h_1+l_2h_2+l_3h_3)] \times \sin[\pi(1+4C(La)^{-3})(l_1h_1+l_2h_2+l_3h_3)]\}^2, \quad (2)$$

where $\mathbf{r}=(l_1\mathbf{a}_1+l_2\mathbf{a}_2+l_3\mathbf{a}_3)/2$ and the $\mathbf{a}$'s are triplet vectors of the unit cell, $\boldsymbol{\kappa}=2\pi(h_1\mathbf{b}_1+h_2\mathbf{b}_2+h_3\mathbf{b}_3)$ and the $\mathbf{b}$'s are the triplet vector set reciprocal to the $\boldsymbol{a}$'s, and $L^2=l_1^2+l_2^2+l_3^2$. The l's are all odd and their limits are determined by the condition $l_1^2+l_2^2+l_3^2\leq L^2(\varepsilon)$. Table 1 gives the values of ε, $R(\varepsilon)$, $L^2(\varepsilon)$, and the number of atoms in the sum, $N(\varepsilon)$, for the eight cases considered. For each of the eight cases the diffuse intensity was computed for $4Ca^{-3}=0{\cdot}15$ and $0{\cdot}90$. In the rest of the paper Figures or Tables with an (*a*) or (*b*) refer to these two values, respectively.

Table 1. *Values of the truncation parameter and related quantities*

Case	ε	$R(\varepsilon)/a$	$L^2(\varepsilon)$	$N(\varepsilon)$
1	$5{\cdot}0000\times10^{-1}$	0·866	3	8
2	$1{\cdot}3636\times10^{-1}$	1·658	11	32
3	$4{\cdot}2857\times10^{-2}$	2·958	35	136
4	$1{\cdot}6484\times10^{-2}$	4·770	91	480
5	$6{\cdot}1728\times10^{-3}$	7·794	243	2008
6	$2{\cdot}4000\times10^{-3}$	12·500	625	8144
7	$9{\cdot}3750\times10^{-4}$	20·000	1600	33552
8	$3{\cdot}7202\times10^{-4}$	31·749	4032	134016

The diffuse intensity was computed at all points h_1h_2 modulo 0·02 for $0\leq h_1\leq 1{\cdot}5$, $0\leq h_2\leq 1{\cdot}5$, and $h_3=0$ on a Control Data CDC 6600 computer using a contour routine to plot iso-diffuse intensity contours. The scattering for cases 2, 4, 6, and 8 is pictured in Figs. 1, 2, 3, and 4, respectively. The contour interval in all Figures (*a*) is 0·1 and is 0·5 in all Figures (*b*). All Figures contain 100 contours. Looking at Fig. 1 through Fig. 4 one sees pronounced ripples in the diffuse scattering. These ripples are due to termination effects and the magnitude of their wavelength (in $|h|$) can be estimated from $\lambda_{|h|}\simeq 2/|L|$. In Fig. 1 through Fig. 4 these termination wavelengths are approximately 0·5, 0·17, 0·08 and 0·03, respectively. Values of the diffuse intensity are listed in Tables 2(*a*) and 2(*b*) for selected points h_1h_20 in reciprocal space. The first eight columns of the Tables list values of the scattering as ε, the truncation parameter, is decreased, or the number of atoms in the sum is increased. It is difficult to discern a clear pattern of convergence. The scattering at the points 0·5,0·5,0 and 1·5,0·5,0 is remarkably insensitive to the number of terms retained in the sum for either value of the strength. The intensity at the point 1·30, 1·30, 0 is insensitive to the number of terms for the larger strength, but oscillates by several orders of magnitude for the smaller strength. For points near the Bragg reflections the intensity increases as the number of terms increases. Unless the termination wavelength is several times less than the distance from the Bragg reflection the calculated intensity cannot be expected to be representative of the true value. In general the oscillations in the scattering values settle down as ε decreases or the number of terms increases, and the relative difference between the intensities in columns seven and eight is less than 15 %.

As equations (1) and (2) stand there is a problem of convergence, and it is in fact not possible to prove in general that the sum converges. At large distances we see that the magnitude of the terms decreases as r^{-2}, but the number of terms increases as r^2. However, if one averages equation (1) or equation (2) over a small volume of κ space the resulting expression can be shown to converge. In fact, any experimental measurement has some finite resolution which performs such an average. Let us illustrate this by assuming a Gaussian resolution function, $(2\pi\sigma^2)^{-3/2}\exp[(\boldsymbol{\kappa}-\boldsymbol{\kappa}_0)^2/2\sigma]$. The average intensity at $\boldsymbol{\kappa}_0$ can be written

$$\langle I(\kappa_0)\rangle \propto |\langle A\rangle|^2+(\langle|A|\rangle^2-|\langle A\rangle|^2) \quad (3)$$

where

$$|\langle A\rangle|^2=\Big|1+\sum_{r\neq0}^{R(\varepsilon)}\exp\{-[r(1+Cr^{-3})]^2\sigma^2/2 +i\boldsymbol{\kappa}_0.\mathbf{r}(1+Cr^{-3})\}-\exp\{-(r\sigma)^2/2+i\boldsymbol{\kappa}_0.\mathbf{r}\}\Big|^2. \quad (4)$$

So long as $[2Cr^{-3}+(Cr^{-3})^2](r\sigma)^2/2\ll 1$, which it always is for any sensible defect strength and resolution breadth, we can neglect the difference in the exponentials quadratic in r and write

$$|\langle A\rangle|^2=\Big|1+\sum_{r\neq0}^{R(\varepsilon)}\exp\{-(r\sigma)^2/2\}\exp\{i\boldsymbol{\kappa}_0\cdot\mathbf{r}\} \times(\exp\{iC\boldsymbol{\kappa}_0\cdot\mathbf{r}/r^3\}-1)\Big|^2. \quad (5)$$

Equation (5) corresponds to averaging the scattering amplitude and then squaring rather than averaging the intensity. However, equation (5) is clearly convergent. Equation (5) differs from equation (1) only by the factor $\exp\{-(r\sigma)^2/2\}$, which is very easy to include in a computer program capable of computing equation (1). The additional terms in equation (3), which are a correction to $|\langle A\rangle|^2$ so that the result is an average intensity, are

$$\begin{aligned}(\langle|A|^2\rangle-|\langle A\rangle|^2)=\sum_r\sum_{r'}&[\exp\{-[(r+Cr/r^3)^2\\&+(r'+Cr'/r'^3)^2]\sigma^2/2\}[\exp\{\mathbf{r}.\mathbf{r}'(1+C/r^3)\\&\times(1+C/r'^3)\sigma^2\}-1]\exp\{iC\boldsymbol{\kappa}_0.(\mathbf{r}/r^3-\mathbf{r}'/r'^3)\}\\&+\exp\{-(r^2+r'^2)\sigma^2/2\}[\exp\{\mathbf{r}.\mathbf{r}'\sigma^2\}-1]\\&-\exp\{-[r^2+(r'+Cr'/r'^3)^2]\sigma^2/2\}\\&\times[\exp\{\mathbf{r}\cdot\mathbf{r}'(1+C/r'^3)\sigma^2\}-1]\exp\{iC\boldsymbol{\kappa}_0.\mathbf{r}'/r'^3\}\\&-\exp\{-[(r+Cr/r^3)^2+r'^2]\sigma^2/2\}\\&\times[\exp\{\mathbf{r}.\mathbf{r}'(1+C/r^3)\sigma^2\}-1]\exp\{iC\boldsymbol{\kappa}_0\cdot\mathbf{r}/r^3\}]\\&\times\exp\{i\boldsymbol{\kappa}_0.(\mathbf{r}-\mathbf{r}')\}.\end{aligned} \quad (6)$$

Table 2(*a*). *Values of* $I(h_1h_20)$ *for selected values of* h_1 *and* h_2, $4Ca^{-3}=0{\cdot}15$

(Numbers in parenthesis are powers of 10).

h_1	h_2	$\varepsilon=5{\cdot}00\ (-1)$	$\varepsilon=1{\cdot}36\ (-1)$	$\varepsilon=4{\cdot}29\ (-2)$	$\varepsilon=1{\cdot}65\ (-2)$	$\varepsilon=6{\cdot}17\ (-3)$	$\varepsilon=2{\cdot}40\ (-3)$	$\varepsilon=9{\cdot}38\ (-4)$	$\varepsilon=3{\cdot}72\ (-4)$	Equation (5)	Equation (10)	Zone
0·50	0	7·59 (−2)	1·43 (−1)	1·52 (−1)	1·92 (−1)	1·95 (−1)	2·26 (−1)	1·97 (−1)	1·92 (−1)	1·98 (−1)	8·64 (−1)	000
											8·64 (−1)	100
0·70	0	4·77 (−2)	2·54 (−2)	5·77 (−3)	1·07 (−3)	2·32 (−4)	1·54 (−2)	3·27 (−3)	1·85 (−3)	1·89 (−3)	1·07 (−1)	100
0·80	0	1·51 (−1)	7·82 (−2)	1·25 (0)	7·63 (−1)	7·30 (−1)	6·37 (−1)	5·95 (−1)	5·44 (−1)	5·93 (−1)	2·86 (−1)	100
0·90	0	4·89 (−1)	2·22 (−2)	1·35 (0)	8·49 (0)	1·54 (1)	6·45 (0)	9·65 (0)	8·41 (0)	9·15 (0)	9·21 (0)	100
0·94	0·08	7·99 (−1)	3·51 (−1)	1·62 (−2)	1·29 (0)	2·75 (0)	8·26 (−1)	1·40 (0)	1·15 (0)	1·32 (0)	1·54 (0)	100
1·06	0·08	2·09 (0)	3·70 (0)	8·78 (0)	1·92 (1)	2·61 (1)	1·64 (1)	1·98 (1)	1·84 (1)	1·93 (1)	1·71 (1)	100
1·10	0	2·69 (0)	5·55 (0)	1·58 (1)	3·73 (1)	5·38 (1)	3·18 (1)	4·01 (1)	3·70 (1)	3·89 (1)	3·52 (1)	100
1·20	0	4·70 (0)	1·00 (1)	1·93 (1)	1·61 (1)	1·59 (1)	1·52 (1)	1·49 (1)	1·45 (1)	1·49 (1)	1·09 (1)	100
1·30	0	6·98 (0)	1·08 (1)	9·66 (0)	9·21 (0)	8·67 (0)	1·03 (1)	9·48 (0)	9·32 (0)	9·32 (0)	5·06 (0)	100
1·50	0	9·92 (0)	8·08 (0)	7·89 (0)	7·09 (0)	7·03 (0)	6·52 (0)	7·00 (0)	7·10 (0)	7·00 (0)	1·47 (0)	100
0·50	0·50	1·14 (0)	1·12 (0)	1·13 (0)	1·12 (0)	1·12 (0)	1·12 (0)	1·12 (0)	1·12 (0)	1·17 (0)	1·17 (0)	000
											1·00 (0)	100
											8·47 (−1)	110
0·70	0·70	3·98 (0)	4·36 (0)	3·14 (0)	3·60 (0)	3·21 (0)	3·52 (0)	3·49 (0)	3·59 (0)	3·60 (0)	1·83 (0)	110
0·80	0·80	4·15 (0)	8·50 (0)	8·71 (0)	6·44 (0)	6·49 (0)	7·46 (0)	7·53 (0)	7·32 (0)	7·27 (0)	4·95 (0)	110
0·92	0·92	2·07 (0)	5·39 (0)	1·85 (1)	4·38 (1)	4·57 (1)	3·37 (1)	3·32 (1)	3·93 (1)	3·72 (1)	3·70 (1)	110
1·00	0·90	1·37 (0)	2·87 (0)	8·94 (0)	2·24 (1)	3·30 (1)	1·90 (1)	2·43 (1)	2·23 (1)	2·35 (1)	2·54 (1)	110
1·10	1·00	5·99 (−2)	2·47 (−1)	4·56 (0)	1·83 (1)	3·02 (1)	1·45 (1)	2·02 (1)	1·80 (1)	1·93 (1)	1·55 (1)	110
1·08	1·08	1·93 (−6)	1·25 (0)	1·20 (1)	3·79 (1)	3·97 (1)	2·69 (1)	2·63 (1)	3·28 (1)	3·06 (1)	2·47 (1)	110
1·20	1·20	5·18 (−1)	3·86 (0)	3·83 (0)	1·82 (0)	1·86 (0)	2·68 (0)	2·74 (0)	2·55 (0)	2·52 (0)	6·99 (−1)	110
1·30	1·30	3·52 (−1)	4·39 (−1)	9·46 (−3)	1·04 (−1)	1·73 (−2)	8·20 (−2)	7·41 (−2)	1·04 (−1)	1·07 (−1)	1·19 (−1)	110
1·50	1·50	2·49 (0)	2·30 (0)	2·35 (0)	2·34 (0)	2·34 (0)	2·34 (0)	2·34 (0)	2·34 (0)	2·34 (0)	1·53 (0)	110
1·30	1·00	4·79 (−1)	1·84 (0)	1·37 (0)	1·20 (0)	1·01 (0)	1·60 (0)	1·30 (0)	1·24 (0)	1·24 (0)	6·18 (−2)	110
0·90	0·50	2·95 (0)	2·51 (0)	2·57 (0)	2·43 (0)	2·32 (0)	2·35 (0)	2·35 (0)	2·35 (0)	2·38 (0)	1·08 (0)	100
											1·17 (0)	110
1·20	0·50	2·19 (0)	1·63 (0)	1·85 (0)	1·82 (0)	1·63 (0)	1·76 (0)	1·74 (0)	1·71 (0)	1·72 (0)	1·12 (0)	100
											1·00 (0)	110
1·50	0·50	6·49 (−1)	6·81 (−1)	6·74 (−1)	6·74 (−1)	6·74 (−1)	6·74 (−1)	6·74 (−1)	6·74 (−1)	6·74 (−1)	7·07 (−1)	100
											1·17 (0)	110

Table 2(*b*). *Values of* $I(h_1h_20)$ *for selected values of* h_1 *and* h_2, $4Ca^{-3}=0{\cdot}90$

(Numbers in parenthesis are powers of 10.)

h_1	h_2	$\varepsilon=5{\cdot}00\,(-1)$	$\varepsilon=1{\cdot}36\,(-1)$	$\varepsilon=4{\cdot}29\,(-2)$	$\varepsilon=1{\cdot}65\,(-2)$	$\varepsilon=6{\cdot}17\,(-3)$	$\varepsilon=2{\cdot}40\,(-3)$	$\varepsilon=9{\cdot}38\,(-4)$	$\varepsilon=3{\cdot}72\,(-4)$	Equation (5)	Equation (10)	Zone
0·50	0	9·87 (0)	6·44 (0)	6·11 (0)	4·75 (0)	4·66 (0)	3·84 (0)	4·61 (0)	4·77 (0)	4·60 (0)	3·31 (−1)	000
											3·31 (−1)	100
0·70	0	4·70 (0)	2·21 (1)	1·91 (1)	1·66 (1)	1·44 (1)	2·14 (1)	1·79 (1)	1·72 (1)	1·72 (1)	9·20 (0)	100
0·80	0	8·65 (−2)	1·84 (1)	9·10 (1)	6·67 (1)	6·43 (1)	5·91 (1)	5·67 (1)	5·37 (1)	5·66 (1)	6·73 (1)	100
0·90	0	5·36 (0)	2·02 (−1)	6·55 (1)	3·48 (2)	6·19 (2)	2·74 (2)	3·99 (2)	3·51 (2)	3·79 (2)	5·39 (2)	100
0·94	0·08	1·26 (1)	5·91 (0)	2·19 (0)	5·53 (1)	1·12 (2)	3·71 (1)	5·98 (1)	4·99 (1)	5·69 (1)	1·55 (2)	100
1·06	0·08	4·76 (1)	1·10 (2)	2·93 (2)	6·59 (2)	9·00 (2)	5·60 (2)	6·77 (2)	6·29 (2)	6·61 (2)	3·93 (2)	100
1·10	0	6·61 (1)	1·68 (2)	5·26 (2)	1·27 (3)	1·83 (3)	1·06 (3)	1·35 (3)	1·24 (3)	1·31 (3)	9·36 (2)	100
1·20	0	1·06 (2)	2·54 (2)	5·19 (2)	4·11 (2)	4·08 (2)	3·87 (2)	3·78 (2)	3·66 (2)	3·78 (2)	2·19 (2)	100
1·30	0	1·29 (2)	2·02 (2)	1·58 (2)	1·50 (2)	1·37 (2)	1·75 (2)	1·56 (2)	1·52 (2)	1·52 (2)	7·21 (1)	100
1·50	0	8·07 (1)	5·68 (1)	5·43 (1)	4·21 (1)	4·13 (1)	3·40 (1)	4·08 (1)	4·23 (1)	4·08 (1)	5·17 (0)	100
0·50	0·50	9·88 (0)	8·45 (0)	8·76 (0)	8·73 (0)	8·75 (0)	8·76 (0)	8·76 (0)	8·76 (0)	8·74 (0)	2·18 (0)	000
											1·00 (0)	100
											2·74(−1)	110
0·70	0·70	3·57 (1)	5·10 (1)	2·67 (1)	3·52 (1)	2·79 (1)	3·35 (1)	3·29 (1)	3·48 (1)	3·50 (1)	9·70 (0)	110
0·80	0·80	1·09 (1)	8·12 (1)	9·50 (1)	5·11 (1)	5·25 (1)	6·95 (1)	7·08 (1)	6·70 (1)	6·62 (1)	6·96 (1)	110
0·92	0·92	4·94 (0)	3·80 (0)	1·81 (2)	7·65 (2)	8·28 (2)	5·29 (2)	5·17 (2)	6·66 (2)	6·14 (2)	9·92 (2)	110
1·00	0·90	1·36 (1)	3·76 (0)	2·56 (1)	2·37 (2)	4·65 (2)	1·76 (2)	2·77 (2)	2·38 (2)	2·62 (2)	6·36 (2)	110
1·10	1·00	4·08 (1)	1·46 (2)	5·10 (2)	1·26 (3)	1·82 (3)	1·05 (3)	1·34 (3)	1·23 (3)	1·30 (3)	8·17 (2)	110
1·08	1·08	4·02 (1)	1·94 (2)	7·92 (2)	1·93 (3)	1·97 (3)	1·43 (3)	1·40 (3)	1·69 (3)	1·59 (3)	1·21 (3)	110
1·20	1·20	1·04 (1)	8·28 (1)	6·37 (1)	2·13 (1)	2·13 (1)	3·94 (1)	4·07 (1)	3·65 (1)	3·59 (1)	1·00 (2)	110
1·30	1·30	5·04 (0)	1·19 (1)	4·06 (1)	2·62 (1)	3·85 (1)	2·78 (1)	2·88 (1)	2·56 (1)	2·51 (1)	8·57 (0)	110
1·50	1·50	8·05 (1)	4·94 (1)	5·62 (1)	5·54 (1)	5·59 (1)	5·60 (1)	5·61 (1)	5·60 (1)	5·60 (1)	5·91 (0)	110
1·30	1·00	4·01 (1)	8·96 (1)	5·99 (1)	5·48 (1)	4·69 (1)	7·05 (1)	5·85 (1)	5·61 (1)	5·64 (1)	4·21 (1)	110
0·90	0·50	1·81 (1)	1·29 (1)	1·33 (1)	1·14 (1)	9·92 (0)	1·03 (1)	1·03 (1)	1·03 (1)	1·08 (1)	1·50 (0)	100
											2·19 (0)	110
1·20	0·50	2·23 (−1)	3·19 (0)	1·40 (0)	1·52 (0)	2·80 (0)	1·90 (0)	1·97 (0)	2·20 (0)	2·14 (0)	1·80 (0)	100
											1·01 (0)	110
1·50	0·50	9·82 (0)	6·02 (0)	6·83 (0)	6·74 (0)	6·80 (0)	6·81 (0)	6·81 (0)	6·81 (0)	6·79 (0)	2·15 (−3)	100
											2·18 (0)	110

The presence of the Gaussian factors in equation (6) assures convergence. Evalution of these contributions on the computer proved too costly and we omitted them. Since we did not compute these contributions we do not know for certain the importance of their contribution. However, if σ vanishes their contribution vanishes since the bracketed terms each vanish. Those terms for which $-1 \ll \mathbf{r}.\mathbf{r}'\sigma^2 \ll 1$ make a small contribution since the bracketed terms are small. If $\mathbf{r}.\mathbf{r}'\sigma^2 \ll -1$, then the Gaussian factors in each term are small. If $\mathbf{r}\cdot\mathbf{r}'\sigma^2 \simeq (r^2+r'^2)\sigma^2/2 \gg 1$, the vectors $\mathbf{r}$ and $\mathbf{r}'$ are nearly equal, and their displacements are nearly equal and small. The first two positive terms are then largely cancelled by the latter two negative terms.

If we examine the squaring operation in either equation (1) or (2) we see that the summation enters in both linearly and quadratically. The linear term we call the size-effect scattering and the quadratic term the Huang (1947) scattering after Borie (1957, 1959). Removing the truncation ripples in $|\langle A\rangle|^2$ with equation (5) means that the truncation ripples in the size-effect term are properly accounted for. It is important to recognize that the omitted terms in equation (6) involve corrections to the Huang scattering only.

We chose $\sigma = 0{\cdot}0636$ which corresponds to an exceedingly good resolution in diffuse-scattering measurements. Now σ has the dimensions of a reciprocal length corresponding to a resolution length $R(\sigma) = 1/\sigma = 15{\cdot}9a$. The results of treating case eight, for which $R(\varepsilon) = 31{\cdot}8a$, according to equation (5) are plotted in Fig. 5. For these values of $R(\sigma)$ and $R(\varepsilon)$ the last term in the sum is reduced by $\exp\{-2\}$. Although the resolution is only partially accounted for, the smoothing effect in Fig. 5 is quite pronounced. The ninth column of Tables 2(*a*) and 2(*b*) lists values for the scattering in case eight according to equation (5). The values of the scattering in this columns are generally a compromise of the values in the preceding two columns.

We have seen that even when the truncation parameter lies between $3{\cdot}72$ and $9{\cdot}38 \times 10^{-4}$ the relative ripple in the diffuse intensity readily accessible to measurement is of the order of 15%. These ripples are clearly visible in Figs. 3 and 4 and in Tables 2(*a*) and 2(*b*). Further, all of the terms neglected are approximately described by a ripple of wavelength $\lambda_\kappa \simeq 2\pi/R(\varepsilon)$. We believe a few final qualitative remarks should be made about dropping terms such as those in equation (6) when a resolution function is taken into account. If the researcher has knowledge of the resolution function to be employed in his measurement then a parameter like $R(\sigma)$ is defined. The factor $\pi^{-1}R(\varepsilon)/R(\sigma)$ determines approximately the number of termination ripples which are averaged by his resolution function. In our example $R(\varepsilon)/R(\sigma) = 2$. Let $\langle A(\kappa)\rangle$ be the scattering amplitude calculated by retaining all terms up to $R(\varepsilon)$ averaged over a resolution function $f(\kappa' - \kappa)$. For our Gaussian resolution function $\langle A(\kappa)\rangle$ is that in equation (5). Since this average removes the ripple in the amplitude given approximately by $B\exp\{i\kappa R(\varepsilon)\}$, we write our scattering amplitude, including the ripple as $\langle A(\kappa)\rangle + B\exp i\kappa R(\varepsilon)$. The relative ripple in the amplitude is $B/\langle A(\kappa)\rangle$. We write for the intensity,

$$I(\kappa) \propto |\langle A(\kappa)\rangle|^2 \left[1 + 2\left|\frac{B}{\langle A(\kappa)\rangle}\right| \times \cos(\kappa R(\varepsilon) + \theta) + \left|\frac{B}{\langle A(\kappa)\rangle}\right|^2\right]. \quad (7)$$

The relative amplitude of the ripple in the intensity as seen in Fig. 3 or 4 is then $2|B|/|\langle A(\kappa)\rangle|$, or just twice that in the amplitude itself. Now assuming that the average amplitude varys much more slowly with κ than the term representing the ripple, we write for the intensity at κ_0 when averaged over the resolution function

$$\langle I(\kappa_0)\rangle \propto |\langle A(\kappa_0)\rangle|^2 \left[1 + 2\left|\frac{B}{\langle A(\kappa_0)\rangle}\right| \times \langle \cos(\kappa R(\varepsilon) + \theta)\rangle + \left|\frac{B}{\langle A(\kappa_0)\rangle}\right|^2\right]. \quad (8)$$

Now the second term within the brackets in equation (8) is twice the average of the relative ripple, and is small compared to unity. The last term represents approximately the relative difference between $\langle I(\kappa_0)\rangle$ and $|\langle A(\kappa_0)\rangle|^2$. In particular, for our Gaussian resolution function equation (8) becomes

$$\langle I(\kappa_0)\rangle \propto |\langle A(\kappa_0)\rangle|^2 \left[1 + 2\left|\frac{B}{\langle A(\kappa_0)\rangle}\right| \times \exp\{-[R(\varepsilon)/R(\sigma)]^2/2\} \times \cos(\kappa_0 R(\varepsilon) + \theta) + \left|\frac{B}{\langle A(\kappa_0)\rangle}\right|^2\right], \quad (9)$$

where $\exp\{-[R(\varepsilon)/R(\sigma)]^2/2\} = \exp\{-2\}$. Comparing columns eight and nine of Tables 2(*a*) and 2(*b*), we estimate $|B|/|\langle A(\kappa_0)\rangle|$ to be generally less than 0·05. Therefore, the relative difference between $\langle I(\kappa_0)\rangle$ and $|\langle A(\kappa_0)\rangle|^2$ is about 0·3%.

Let us compare the preceding results for the diffuse scattering with an approximation that is often used to compute the scattering from defects. We treat $\boldsymbol{\kappa}.\boldsymbol{\mu}_n$ as a small quantity, write $i\boldsymbol{\kappa}.\boldsymbol{\mu}_n$ for $(\exp\{i\boldsymbol{\kappa}.\boldsymbol{\mu}_n\} - 1)$, and use Ewald's integral transformation formula, while retaining only the first term (Ewald, 1938; Ekstein, 1945; Cochran, 1956) and write

$$I(\kappa) \propto \left[1 - \frac{2(-1)^{H+K+L}C}{a^3}\left(\frac{Hn_1 + Kn_2 + Ln_3}{n_1^2+n_2^2+n_3^2} + 1\right) \times \frac{\sin 2\pi(r_0/a)(n_1^2+n_2^2+n_3^2)^{1/2}}{(r_0/a)(n_1^2+n_2^2+n_3^2)^{1/2}}\right]^2. \quad (10)$$

H, K, and L are the usual Miller indices. The n's define a vector $\mathbf{g} = 2\pi(n_1\mathbf{b}_1 + n_2\mathbf{b}_2 + n_3\mathbf{b}_3)$ from the reciprocal lattice point H, K, L to $\boldsymbol{\kappa}$. In Ewald's formula the second term in the bracket is to be summed over all H, K, L.

In practice only the contribution from the nearest H, K, L is considered. Here $r_0=(3a/2)^{1/2}$. The diffuse intensity was computed at all points n_1, n_2 and n_3 modulo 0·02 for $-\frac{1}{2}\leq n_1\leq\frac{1}{2}$, $-\frac{1}{2}\leq n_2\leq\frac{1}{2}$, and $n_3=0$ about the reflections 000, 100, and 110. A contour routine was used to plot iso-diffuse intensity contours within these zones. These zones were joined together in a composite covering the same region of reciprocal space as previously considered. The results are pictured in Fig. 6. Column ten in Tables 2(*a*) and 2(*b*) gives values of the diffuse intensity using this approximate method [equation (10)]. Some points h_1h_2 are common to two or more zones and the particular zone is identified in column eleven. For instance the point 0·5, 0·5 can be calculated from three different zones. The agreement amongst the different zones is poor especially in Table 2(*b*). In Table 2(*a*) equation (10) gives values of the scattering close to the Bragg reflections in reasonable agreement with the preceding three columns. The agreement in Table 2(*b*) is considerably poorer. The diffuse scattering contours in Fig. 6(*a*) and (*b*) are similar in shape, while there is considerable difference in contour shape between the (*a*) and (*b*) parts of the other Figures. The reason for similarity in Fig. 6 is apparent from the form of equation (10). The second term is directly proportional to the strength. However, in equation (1), (2) or (5) the proportionality is in the argument of a circular function, and as the strength becomes large the contour shapes are altered, whereas in equation (10) they are only scaled.

3. Summary

We have shown that when the truncation parameter $\varepsilon<10^{-3}$ the diffuse scattering calculated according to the sum formulation is reasonably stationary to within $\sim 15\,\%$ in a region of reciprocal space readily accessible to measurement. The instability of the calculated scattering is associated with a termination ripple whose wavelength $\lambda_\kappa\simeq 2\pi/R(\varepsilon)$. The stability can be improved by taking into account the finite resolution of any measurement. In this case $R(\varepsilon)$ should be chosen larger than twice the resolution distance $R(\sigma)$. While the expression for the intensity should be averaged over the resolution function, the computational procedures are costly, and we have given qualitative arguments for using the average over the amplitude instead. Finally, we have compared a commonly used approximation for the diffuse scattering with the sum formulation. As long as $\boldsymbol{\kappa}.\boldsymbol{\mu}_n$ is small, then the approximation is in reasonable agreement with the sum formulation near the Bragg reflections. When this criterion is not well satisfied the agreement diverges.

In conclusion we would like to say a few words about the size-effect term. If the strength of the defect is small then this term produces an asymmetry in the diffuse scattering about the Bragg reflections. For the model considered, if the sum of the Miller indices is even the scattering will be largest on the side of the reflection toward the origin of reciprocal space while if odd the reverse is true. This comes about because of the reinforcement or cancellation of the Huang scattering by the size-effect term. If the sign of the strength of the defect were not known it could be deduced from the size-effect term. However, the Huang scattering is always larger on the side of the reflection further from the origin. If the defect strength is large then the Huang term dominates the diffuse scattering and the intensity will always appear larger on the far side of a reflection as in the (*b*) parts of the Figures.

The authors wish to express their thanks to Miss Estarose Wolfson and Mrs Margaret Hind, for programming the scattering equations on the Control Data 6600, and to Messrs Harry Maile and Emil Caiazza for preparation of the Figures.

References

BORIE, B. S. (1957). *Acta Cryst.* **10**, 89.
BORIE, B. S. (1959). *Acta Cryst.* **12**, 280.
COCHRAN, W. (1956). *Acta Cryst.* **9**, 259.
EKSTEIN, H. (1945). *Phys. Rev.* **68**, 120.
ESHELBY, J. D. (1954). *J. Appl. Phys.* **25**, 255.
EWALD, P. P. (1938). *Göttinger Nachrichten*, **3**, 55.
GOLAND, A. N. & KEATING, D. T. (1968). *J. Phys. Chem. Solids*, **29**, 785.
HUANG, K. (1947). *Proc. Roy. Soc.* A**190**, 102.
KEATING, D. T. (1968). *J. Phys. Chem. Solids*, **29**, 771.
MARTIN, D. G. (1960). *Phil. Mag.* **5**, 1235.